Narrowing the Length Distribution of Ge Nanowires

V. G. Dubrovskii,[1,2] T. Xu,[3] Y. Lambert,[3] J.-P. Nys,[3] B. Grandidier,[3,*] D. Stiévenard,[3] W. Chen,[4] and P. Pareige[4]

[1]St. Petersburg Academic University, Khlopina 8/3, 194021 St. Petersburg, Russia
[2]Ioffe Physical Technical Institute of the Russian Academy of Sciences, Politekhnicheskaya 26, 194021 St. Petersburg, Russia
[3]Institut d'Electronique, de Microélectronique et de Nanotechnologie, IEMN-CNRS (UMR 8520), Département ISEN, 41 bd Vauban, 59046 Lille Cedex, France
[4]Groupe de Physique des Matériaux, Université de Rouen, CNRS UMR 6634, Av. de l'Université, BP 12, 76801 Saint Etienne du Rouvray, France

(Received 3 June 2011; revised manuscript received 9 December 2011; published 5 March 2012)

Synthesis of nanostructures of uniform size is fundamental because the size distribution directly affects their physical properties. We present experimental data demonstrating a narrowing effect on the length distribution of Ge nanowires synthesized by the Au-catalyzed molecular beam epitaxy on Si substrates. A theoretical model is developed that is capable of describing this puzzling behavior. It is demonstrated that the direction of the diffusion flux of sidewall adatoms is size dependent and has a major effect on the growth rate of differently sized nanowires. We also show that there exists a fundamental limitation on the maximum nanowire length that can be achieved by molecular beam epitaxy where the direction of the beam is close to the growth axis.

DOI: 10.1103/PhysRevLett.108.105501 PACS numbers: 81.07.Gf, 68.70.+w, 81.10.Aj

Self-assembly of materials at the nanometer scale is an attractive approach because a large number of similar nanostructures can be grown simultaneously. A fundamental issue that is common to the growth of all self-assembled systems is the understanding of physical mechanisms governing the size distribution of nanostructures [1,2]. Indeed, numerous applications rely on the fabrication of nanostructures with a rather narrow size distribution. For example, obtaining a monodisperse ensembles of colloid particles has been one of the key issues in forming the superlattice structures that can support high-density magnetization reversal transitions [3] or feature an enhanced strength and robustness [4]. The stability of nanoparticle dispersions to prepare highly insoluble drugs is strongly affected by the initial size distribution of the nanoparticles [5]. Laser and photonic applications based on the arrays of self-assembled semiconductor quantum dots and nanowires (NWs) also critically depend on their size uniformity [6,7].

Scaling behavior of the size distribution has been found for the growth of nanostructures in the aggregation regime, where the incoming material penetrates into the existing islands only [8,9]. However, more complex atomic processes can be involved, including the reevaporation of atoms, their dissolution into the substrate and change in potential gradients that affect surface diffusion. As a result, the strategies to narrow the size distribution of nanostructures are rather scarce [10]. Here, we focus on the length distribution of Ge NWs grown from Au seed particles by molecular beam epitaxy (MBE). The analysis of NW length as a function of their diameter with time shows an unexpected behavior that enables a narrowing of their length distribution whatever the initial particle size is. We develop a model that explains the observed behavior. It reveals how important the magnitude and directions of the adatom diffusion flux on the NW sidewalls is to tailor the length of semiconductor NWs grown by MBE.

The Au seed particles and Ge NWs were fabricated as described in Refs. [11,12]. In brief, the Au droplets were formed directly by Au deposition onto a heated Si(111) surface in an ultra high vacuum chamber. The growth of Ge NWs was then achieved by the sublimation of Ge at a deposition pressure of 10^{-9} mbar. In our MBE system, the Ge beam is perpendicular to the substrate, and the substrate is not rotated during growth. The equivalent deposition rate V in all growth runs was 0.18 ± 0.02 nm/s. The Si(111) substrate was heated at 350 °C, which has been found to be the best growth temperature to obtain long and regular ⟨110⟩-oriented Ge NWs [13]. The growth duration was varied up to 70 min. The NW morphology was then investigated by scanning electron microscopy (SEM).

The inset of Fig. 1 shows a SEM image of a typical ⟨110⟩-oriented Ge NW that points at 54.7° from the surface plane above the Ge overgrown layer, consistent with previous studies [12,14]. Approximating the irregular hexagonal cross section of the NW with a disk of radius R, the measurement of the NW radius yields 90 nm, while the NW length L above the surface plane is 930 nm. As the formation of Au droplets leads to a significant variation in the size of the seed particles, a statistical analysis of the distribution of the NW length as a function of the radius was performed for different growth times. Figure 1 reveals a decreasing $L(R)$ dependence for a growth time of 15 min, which is the hallmark of a diffusion-induced (DI) growth [15,16].

At the longest growth times studied in this work, an opposite behavior is observed: L increases with R. Such an

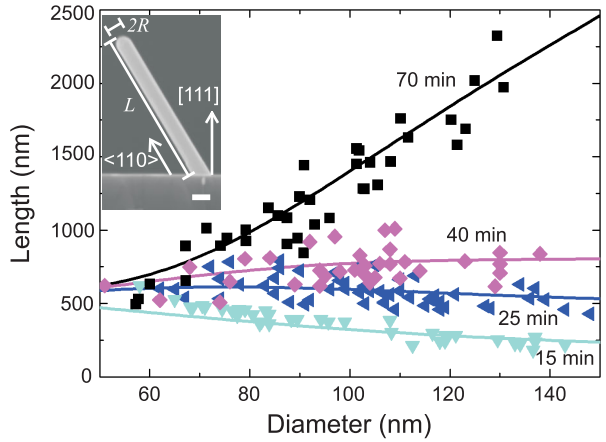

FIG. 1 (color online). Experimental (symbols) length-diameter dependences of ⟨110⟩-oriented Ge NWs obtained for different growth times. Solid lines are theoretical fits obtained from Eq. (4) with the parameters summarized in Table I. Inset: SEM image of a ⟨110⟩-oriented Ge NWs grown at 350 °C. L and R yield for the NW length above the Ge layer and the NW radius, respectively. Scale bar is 100 nm.

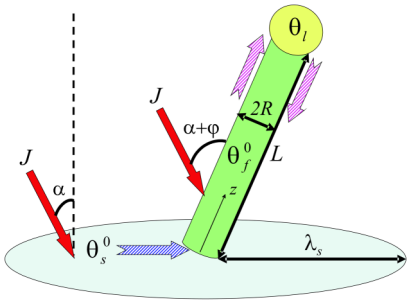

FIG. 2 (color online). Illustration of the model with the parameters described in the text. The cross-hatched arrows indicate the direction of the adatom fluxes that depend on the magnitude of the surface, sidewall, and droplet activities, θ_s^0, θ_f^0, and θ_l.

increasing length-diameter curve is usually explained by the Gibbs-Thomson (GT) effect [17]. As demonstrated in Refs. [18,19], the $L(R)$ curves of Si and III-V NWs may feature both types of dependences at different R. However, to the best of our knowledge, the conversion of decreasing into increasing $L(R)$ dependence for NWs of the same diameters with the growth time is observed here for the first time. As consequence, a growth regime exists, around 30 min, where the length is almost independent of R, leading to a surprising narrowing of the length distribution. This effect has not been noticed in previous studies, and, based on the widespread interest to tailor the length distribution of NWs, its explanation requires a deeper insight into the fundamental mechanisms of NW growth.

It is well known [18–21] that the NW growth chronology critically depends on the magnitudes of adatom diffusion lengths on the substrate surfaces $\lambda_s = \sqrt{D_s \tau_s}$, and on the sidewall facets (f) $\lambda_f = \sqrt{D_f \tau_f}$, with D and τ being the diffusion coefficients and the effective lifetimes of the corresponding surfaces. Whenever $\lambda_f \gg L$, all surface adatoms that migrate to the NW base will subsequently reach its top. Taking J as the adatom arrival rate from the beam with the incident angle α, while φ is the NW tilt angle (see Fig. 2), the effective activities of Ge adatoms on the substrate $\theta_s^0 = \chi_s J \cos\alpha \sigma_s \tau_s$ and sidewall facets $\theta_f^0 = (\chi_f/\pi) J \sin(\alpha + \varphi) \sigma_f \tau_f$ [19] must match around the NW base, when $\lambda_s \gg R$. In these expressions, χ are the accommodation coefficients, and σ the elementary areas on the corresponding surfaces.

The dependence of concentration of sidewall adatoms at the coordinate z along the NW axis is generally given by the sum of θ_f^0 and a linear combination of two hyperbolic functions of z/λ_f [16–21]. Therefore, at $\lambda_f \gg L$ and $\theta_f(z = 0) = \theta_s^0$, the leading terms of $\theta_f(z)$ in z/λ_f can be written as

$$\theta_f(z) = \theta_s^0 + C(z/\lambda_f) + (1/2)(\theta_l - \theta_f^0)(z/\lambda_f)^2, \quad (1)$$

where $\theta_l = \exp(\mu_l/k_B T)$ is the droplet activity, μ_l is the chemical potential of Ge in the droplet, T is the surface temperature, and k_B is the Boltzmann constant. The constant C is given by the boundary condition $\theta_f(z = L) = \theta_l$.

The variation of the NW length with time in the DI growth mode is related to the derivative of the sidewall activity as follows:

$$\frac{\pi R^2}{\Omega_s}\left(\frac{dL}{dt}\right)_{\text{diff}} = -2\pi R \frac{D_f}{\sigma_f} \frac{\partial \theta_f}{\partial z}\bigg|_{z=L}, \quad (2)$$

where Ω_s is the elementary solid volume.

Using Eqs. (1) and (2), and introducing the deposition rate, $V = J\Omega_s \cos\alpha$, we arrive at the nonlinear growth equation of the form,

$$\frac{1}{V}\frac{dL}{dt} = \frac{a g_f L}{R} + \frac{2\lambda_s^2 g_s}{bLR} + A, \quad (3)$$

where we replace the ratios between different activities by the functions $g_f = \chi_f(1 - \theta_l/\theta_f^0)$ and $g_s = \chi_s(1 - \theta_l/\theta_s^0)$ to better highlight the physical reason at the origin of the narrowing effect. The coefficient $a = \sin(\alpha + \varphi)/(\pi \cos\alpha)$ is the geometrical factor of MBE growth and $b = (D_s \sigma_f / D_f \sigma_s)$ is a constant which is of the order of 1. The A term in Eq. (3) writes as $A = A_{\text{imp}} - 1 - A_{\text{des}}$, describing the direct impingement flux through the Au catalyst, the growth rate of the surface layer between the NWs, and the desorption from the droplet, respectively [16,17,21]. In our case, A_{imp} is very close to 1 and thus is compensated by the surface growth, while A_{des} can be neglected in the first approximation at a low temperature of 350 °C. In the following, we consider Eq. (3) at $A = 0$.

Therefore, the growth rate contains two contributions. The first term describes the growth rate from Ge adatoms directly impinging the sidewalls and migrating to the NW

top. The second one stands for Ge adatoms that first impinge the substrate surface, diffuse to the NW base and then to the top along the sidewalls. The growth chronology of a given NW crucially depends on the signs of coefficients g_f and g_s [20], that are intimately related to the dependence of the droplet activity with R. The simplest approximation for $\theta_l(R)$ is given by $\theta_l = \theta_l^\infty \exp(R_{GT}/R)$ [18–20], with $R_{GT} = (2\gamma\Omega_l \sin\beta)/(k_B T)$ as the GT radius, γ the droplet surface energy, β the contact angle, and θ_l^∞ the R-independent activity of an infinitely large alloy.

As follows from Eq. (3), the DI contributions are positive at $g_f > 0$ and $g_s > 0$, and negative otherwise. In the beginning of growth where L is small, the second term dominates showing that, since the NW is mainly fed by the surface adatoms, it can emerge from the substrate only at $g_s > 0$. In the opposite case of large L, the DI growth is usually assumed to be controlled by a positive L term at $g_f > 0$ [16,18,19,21]. This yields an infinite growth with L increasing exponentially as long as $L \ll \lambda_f$ [21].

Integration of Eq. (3) with the initial condition $L(t = t_0) = 0$, where t_0 is the incubation time required to initiate the NW growth, readily gives

$$L = 2\Lambda_s \sqrt{\frac{\exp[2ag_f V(t - t_0)/R] - 1}{2ag_f}}. \quad (4)$$

Here, $\Lambda_s = \lambda_s\sqrt{g_s/b}$ is the effective diffusion length of surface Ge adatoms which is of the order of λ_s. Obviously, at small t, Eq. (4) can be reduced to the square root law $L = 2\Lambda_s\sqrt{V(t - t_0)/R}$ regardless of g_f. At large t, it gives either an exponential NW elongation when $g_f > 0$, or a limited growth to a finite length $L = \Lambda_s\sqrt{2/(a|g_f|)}$ when $g_f < 0$. Positive and negative directions of the diffusion flux of sidewall adatoms are shown schematically in Fig. 2.

We now turn to the analysis of the $L(R)$ curves for the ⟨110⟩-oriented Ge NWs, with $\alpha = 0$, $\varphi = 35.3°$, and $t_0 = 6$ min. Based on Eq. (4), assuming Λ_s of about 100 nm, which is consistent with previous estimates for the diffusion lengths [18,19,22], we are able to reproduce the experimental variations of L with R for the different growth times (Fig. 1). In order to better capture the manifestation of a narrowing effect, we also plot out the time evolution of L for different R for a larger set of samples than the ones displayed in Fig. 1. As shown in Fig. 3, at the beginning, the narrowest 60 nm-thick NWs grow faster, but then stop growing. Conversely, the thicker NWs that have evolved slowly during the first 30 min overtake the length of the 60 nm-thick NWs to become more than 4 times longer than the narrowest NWs after 70 min of growth. Remarkably, a growth stage exists of around 30 min of growth where the size distribution of ⟨110⟩ Ge NWs is quite narrow, and this effect is well supported by the theoretical curves. In particular, 60 nm-thick NWs clearly exhibit the limited growth to a finite length, while thicker

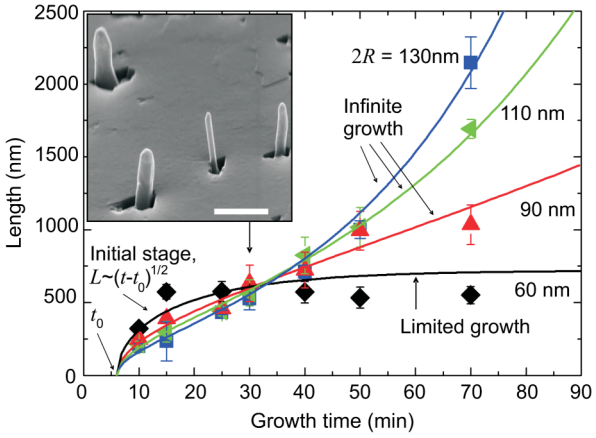

FIG. 3 (color online). Experimental length-time dependences of ⟨110⟩-oriented Ge NWs for four different diameters (symbols), and theoretical fits (lines) obtained from Eq. (4) with the parameters summarized in Table I. Inset: SEM image of ⟨110⟩-oriented Ge NWs grown for a time of 30 min. The scale bar is 600 nm. Different growth regimes are indicated by arrows.

NWs follow the regime of exponential growth in the large time limit.

Crucial to this focusing effect is the value of g_f, as it controls the magnitude and the direction of the corresponding diffusion flux. As seen from Table I, g_f increases from -0.30 for 60 nm diameter NWs (corresponding to a negative diffusion flux from the droplet) to 0.75 for 130 nm diameter NWs. One obvious reason for the increase of g_f and the corresponding $\Delta\mu_{fl} = k_B T \ln(\theta_f/\theta_l)$ values with R is the GT effect [18–20]. We note, however, that the increase of g_f obtained from the fits of ⟨110⟩-oriented NWs is faster than that given by the Arrhenius-like radius dependence of the liquid activity at a constant θ_l^∞. Therefore, the effective supersaturation of sidewall adatoms is influenced by other physical effects, such as (i) variation of the Ge concentration in differently sized droplets, (ii) different atomic structure of sidewalls of differently sized NWs [12], (iii) possible time variation of the Ge percentage caused by the Au migration, and (iv) scattering of the Ge beam from the sidewalls resulting in $\chi_f < 1$. Regardless of physical mechanisms changing the activity of sidewall adatoms, a negative diffusion can be the only explanation for the time-limited NW growth. The slight decrease of length after the

TABLE I. Fitting parameters for differently sized ⟨110⟩-oriented NWs, θ_f^0/θ_l and $\Delta\mu_{fl} = k_B T \ln[\theta_f^0/\theta_l]$ are obtained assuming $\chi_f = 1$.

$2R$ (nm)	g_f	θ_f^0/θ_l	$\Delta\mu_{fl}$ (meV)
60	−0.30	0.77	−14
90	0.13	1.15	7.5
110	0.45	1.82	32
130	0.75	4.0	74

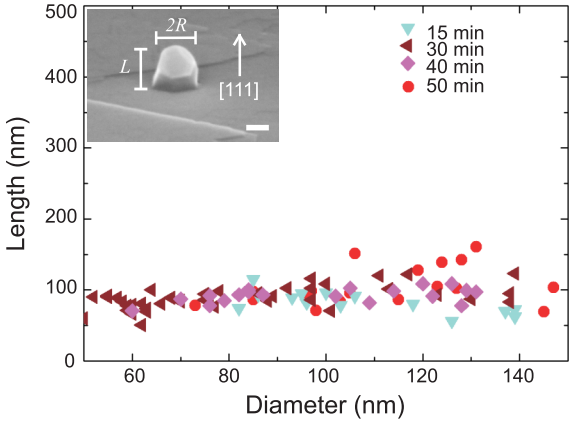

FIG. 4 (color online). Length-diameter dependences of ⟨111⟩-oriented Ge NWs after 15, 30, 40, and 50 min of growth. L and R yield for the NW length above the Ge layer and the NW radius, respectively. Scale bar: 50 nm.

saturation observed for the thinnest ⟨110⟩-oriented NWs in Fig. 3 can be explained by their negative growth via the diffusion from the top to the substrate [20].

Finally, we would like to point out that the narrowing effect is expected to be noticeable only when $\sin(\alpha + \varphi)$ readily differs from zero. As shown in Fig. 4, [111]-oriented Ge NWs also emerge on the Si(111) substrate during growth. Their length is much smaller than the length of the ⟨110⟩-oriented NWs and is found to be almost constant with R and t. When $\sin(\alpha + \varphi)$ tends toward 0, the product ag_f becomes negative regardless of the NW radius: $ag_f = -\theta_l/(J\sigma_f\tau_f) < 0$ and a finite NW length, independent of R and t, is expected, as described above. Therefore, all the [111]-oriented NWs should follow the scenario of limited growth. Such a behavior is consistent with almost invariant L seen in Fig. 4. We suspect this growth regime to occur quickly due to a small diffusion length on the NW sidewalls, as they are highly faceted [12,23]. It is noteworthy that, whenever the liquid activity becomes larger than that of sidewall adatoms, the minimum of chemical potential is reached at the NW sidewalls. This should lead to a radial growth of NWs after the length saturation. A more detailed analysis of ⟨111⟩ Ge NWs will be given elsewhere.

In summary, we have presented experimental data and a theoretical model showing that the Au-catalyzed Ge NWs obtained by MBE on Si(111) substrates exhibit a rather complex growth behavior. Narrow ⟨110⟩ Ge NWs grow faster than wider ones at the beginning, but almost stop growing after a certain growth time. Consequently, the length-time dependences of differently sized NWs cross at a certain time, after which the length-diameter dependences become reversed. Central to this effect is the change in the direction of the flow of adatoms on the NW sidewalls during the growth, due to the droplet activity dependence on the radius of the seed particle. It sets a fundamental limitation on the maximum length of MBE grown NWs, that should be considered as a rather general phenomenon, particularly in the setups where the direction of the beam is close to the substrate normal. However, such a limitation can be used to narrow the length distribution of NWs at a certain time regardless of the initial distribution of growth seeds, which is the main message of this Letter.

This work was partially supported by the contracts with the Russian Ministry of Education and Science, the scientific programs of the Russian Academy of Sciences, the grants of the Russian Foundation for Basic Research, the FP7 projects SOBONA and FUNPROB, and the Direction Générale de l'Armement (DGA) under Contract No. REI-N02008.34.0031.

*bruno.grandidier@isen.iemn.univ-lille1.fr

[1] J. Tersoff, C. Teichert, and M. G. Lagally, Phys. Rev. Lett. **76**, 1675 (1996).
[2] K. Bromann, C. Félix, H. Brune, W. Harbich, R. Monot, J. Buttet, and K. Kern, Science **274**, 956 (1996).
[3] S. Sun, C. B. Murray, D. Weller, L. Folks, and A. Moser, Science **287**, 1989 (2000).
[4] K. E. Mueggenburg, X.-M. Lin, R. H. Goldsmith, and H. M. Jaeger, Nature Mater. **6**, 656 (2007).
[5] Y. Liu, K. Kathan, W. Saad, and R. K. Prud'homme, Phys. Rev. Lett. **98**, 036102 (2007).
[6] S. Fafard, K. Hinzer, S. Raymond, M. Dion, J. McCaffrey, Y. Feng, and S. Charbonneau, Science **274**, 1350 (1996).
[7] O. L. Muskens, S. L. Diedenhofen, B. C. Kaas, R. E. Algra, E. P. A. M. Bakkers, J. G. Rivas, and A. Lagendijk, Nano Lett. **9**, 930 (2009).
[8] Y. Ebiko, S. Muto, D. Suzuki, S. Itoh, K. Shiramine, T. Haga, Y. Nakata, and N. Yokoyama, Phys. Rev. Lett. **80**, 2650 (1998).
[9] R. Ruiz, B. Nickel, N. Koch, L. C. Feldman, R. F. Haglund, A. Kahn, F. Family, and G. Scoles, Phys. Rev. Lett. **91**, 136102 (2003).
[10] X. Peng, J. Wickham, and A. P. Alivisatos, J. Am. Chem. Soc. **120**, 5343 (1998).
[11] T. Xu, J.-P. Nys, B. Grandidier, D. Stiévenard, Y. Coffinier, R. Boukherroub, R. Larde, E. Cadel, and P. Pareige, J. Vac. Sci. Technol. B **26**, 1960 (2008).
[12] T. Xu, J. Sulerzycki, J.-P. Nys, G. Patriarche, B. Grandidier, and D. Stiévenard, Nano. Res. Lett. **6**, 113 (2011).
[13] A. Kramer, M. Albrecht, T. Boeck, T. Remmele, P. Schramm, and R. Fornari, Superlattices Microstruct. **46**, 277 (2009).
[14] .E. F. Pecora, A. Irrera, P. Artoni, S. Boninelli, C. Bongiorno, C. Spinella, and F. Priolo, Electrochem. Solid State Lett. **13**, K53 (2010).
[15] L. Schubert, P. Werner, N. D. Zakharov, G. Gerth, F. M. Kolb, L. Long, U. Gösele, and T. Y. Tan, Appl. Phys. Lett. **84**, 4968 (2004).
[16] V. G. Dubrovskii, G. E. Cirlin, I. P. Soshnikov, A. A. Tonkikh, N. V. Sibirev, Yu. B. Samsonenko, and V. M. Ustinov, Phys. Rev. B **71**, 205325 (2005).

[17] V. G. Dubrovskii, G. E. Cirlin, and V. M. Ustinov, Semiconductors **43**, 1539 (2009).
[18] L. E. Fröberg, W. Seifert, and J. Johansson, Phys. Rev. B **76**, 153401 (2007).
[19] V. G. Dubrovskii, N. V. Sibirev, G. E. Cirlin, I. P. Soshnikov, W. H. Chen, R. Larde, E. Cadel, P. Pareige, T. Xu, B. Grandidier, J.-P. Nys, D. Stievenard, M. Moewe, L. C. Chuang, and C. Chang-Hasnain, Phys. Rev. B **79**, 205316 (2009).
[20] V. G. Dubrovskii, N. V. Sibirev, G. E. Cirlin, A. D. Bouravleuv, Yu. B. Samsonenko, D. L. Dheeraj, H. L. Zhou, C. Sartel, J. C. Harmand, G. Patriarche, and F. Glas, Phys. Rev. B **80**, 205305 (2009).
[21] J. C. Harmand, F. Glas, and G. Patriarche, Phys. Rev. B **81**, 235436 (2010).
[22] V. G. Dubrovskii, N. V. Sibirev, R. A. Suris, G. E. Cirlin, J. C. Harmand, and V. M. Ustinov, Surf. Sci. **601**, 4395 (2007).
[23] T. Xu, J.-P. Nys, A. Addad, O. I. Lebedev, A. Urbieta, B. Salhi, M. Berthe, B. Grandidier, and D. Stiévenard, Phys. Rev. B **81**, 115403 (2010).